16th World Conference on Earthquake, 16WCEE 2017

Santiago Chile, January 9th to 13th 2017

Paper N° 3894

Registration Code: S-E1466019631

Performance assessment of lead rubber bearing system and triple friction pendulum system at Piura's hospital, in Peru

F. Vilca-Cordova [1], L. G. Quiroz [2], M. Torres-Matos[2]

[1] *Graduate Student, Faculty of Civil Engineering, National University of Engineering, Lima-Peru - fic_fico@yahoo.es*
[2] *Associated Researcher, Department of Earthquake Engineering, Japan-Peru Earthquake Engineering and Disaster Mitigation Center, Faculty of Civil Engineering, National University of Engineering, Lima-Peru - lgquiroz@uni.edu.pe*
[2] *Researcher, Department of Earthquake Engineering, Japan-Peru Earthquake Engineering and Disaster Mitigation Center, Faculty of Civil Engineering, National University of Engineering, Lima-Peru - matorresm@gmail.com*

Abstract

The occurrence of earthquakes has caused significant damage to structural and even nonstructural elements. In hospitals, nonstructural components and contents represent around 92% of a building's total cost. As such, every effort must be made to reduce such damage. According to the Peruvian design standard (E.030) [1] for earthquake resistance, hospitals must continue to provide services during and after seismic events in accordance with the principle of earthquake-resistant design.

A good response has been observed in seismic isolation projects during and after earthquakes for the Caraquez Bay Bridge, Ecuador 2016; the Ishinomaki Red Cross Hospital, Japan 2011; the Military Hospital located in Santiago, Chile 2010; and LNG tanks for the Pampa Melchoritam, Peru 2007. In view of this, one approach to reducing damage to structural and nonstructural elements, components and equipment is the use of seismic isolation devices. Seismic isolation systems have already been implemented in some types of structures in Peru such as hospitals, offices, universities and gas storage tanks, and today, seismic isolation systems in accordance with E.030 [1] standards must be used in hospitals.

This study presents an analysis of the performance assessment of a lead rubber bearings system and a triple friction pendulum bearings system at the hospital in Piura. This hospital is located on the northern Peruvian coast in an important city with respect to the economy. It is located in a zone of high seismic activity according to E.030 [1].

Time-history analyses were carried out with nonlinear analytical models taking into account the horizontal components of scaled seismic records obtained from overseas events. Two types of seismic isolation systems at the base of the structure were separately evaluated. The first system was composed of lead rubber bearings (LRB) and the second consisted of triple friction pendulum (TFP) bearings.

The performance of these types of isolators was evaluated in terms of seismic isolator response, average floor acceleration, average inter-story drift and average base shear. Special attention was paid to the performance assessment of both seismic isolation systems. This study found that LRB Systems provided a better average floor acceleration response and hysteresis loops than the TFP Systems for undertaking lower bound analysis, while the TFP Systems had better average floor acceleration response and hysteresis loops than the LRB Systems for undertaking upper bound analysis.

Keywords: Base isolation; LRB; TFP.

1. Introduction

A large part of the world's population lives in regions that are at risk from earthquakes of varying severity and frequency. Earthquakes cause significant economic and human losses every year. Various aseismic construction designs and technologies have been developed over the years in order to mitigate the effects of earthquakes on structures and potentially vulnerable contents.

Seismic isolation is one approach to improving the performance of structural and non-structural elements and contents. It consists mainly of installing mechanisms which decouple the structure, or its contents, from potentially damaging earthquake-induced ground or support movements. This decoupling is achieved by increasing the flexibility of the system and providing suitable damping. In many but not all seismic isolation applications, the mechanism is mounted beneath the structure and is referred to as a base isolation system [2].

One historical seismic isolation structure found in Peru is Machu Picchu. This ‘Temple of the Sun’ was made using dry-stone walls and large stones with smooth and flat surfaces. It would appear that the walls were built to reduce friction during earthquakes by allowing them to move back and forth over their lower foundations without causing any damage [3].

2. Numerical model

2.1 Superstructure System

The Piura hospital is located on the northern coast of Peru. Piura is a site with a high level of seismicity according to E.030 standards. The hospital has 16 blocks. In this research project, block 5 has been analyzed. This block has 5 stories along with a structural lateral resistant system composed of reinforced concrete (RC) frames. Each story has a height of 4.25 meters. The weight of the structure is 185000 kN. The typical floor area is 3665 m^2. A heavy mat foundation system has been used with a depth of 0.70 m, and the type of soil is D according to ASSHTO [4]. Figure 1 shows a plan view of the location of the isolators.

2.2 Triple Friction Pendulum (TFP) System

The behavior of TFP bearings can be represented by five regimes [5]. In this study, a link element known as the “friction isolator” was used as employed by the SAP2000 program [6] to create a bilinear approximation of the multi-linear TFP. This approach was chosen because it is a simple method that represents the conduct of the essential bearing, although this bearing model does not capture the stiffening behavior that occurs near the maximum displacement capacity of the bearing at ‘regimen V’. Analysis was carried out for the properties of upper-bound and lower-bound isolators.

This analysis employs a bilinear approximation that uses an equal area approach that selects the bilinear model yield displacement (u^*_{EQ}) by balancing the hysteresis loop area (Areas 1 and 2), as can be seen in figure 2, which has been gained and lost by the approximation. Figure 2 shows a comparison of the true bearing conduct and the equal area bilinear approximation. The assumptions for modelling TFP bearings were undertaken in accordance with the IBC-SEAOC Structural /Seismic Design Manual [7] and are as follows:

2.2.1 Friction Properties

The friction isolator link element in SAP2000 accepts friction values for fast and slow sliding and a rate parameter that describes the transition between fast and slow sliding. In this study, the fast friction is set equal to the design of outer friction, and the slow friction is set equal to one half of the fast friction. The rate parameter is taken as 2.54 sec-in, and the velocity is assumed to be partitioned equally on the top and bottom of the sliding surfaces of the bearing. This resulted in a rate parameter of 2.54/2 = 1.27 sec-in.

As Figure 2 demonstrates, the yield displacement for the outer sliding surface based on the true bearing conduct, u*, is calculated as

$$u^* = (\mu_{outer} - \mu_{inner})\, x\, R_{eff\ inner} \tag{1}$$

Note: The yield displacement for the inner sliding surface is very small and has been neglected.

The friction coefficient at zero displacement, μ, is calculated as

$$\mu = \mu_{Fast} = \mu_{outer} - u^{*}x\left(\frac{1}{R_{eff\ outer}}\right) \tag{2}$$

$$\mu_{Slow} = \left(\frac{\mu_{Fast}}{2}\right) \tag{3}$$

2.2.2 Non – Linear Stiffness (Horizontal)

This is the initial stiffness, k_i , of the bearing. It is calculated here using the average bearing load.

$$\text{Nonlinear stiffness} = \text{Avg. vertical load x} \left(\frac{\text{Rise}}{\text{Run}}\right) \tag{4}$$

As shown in figure 2, the yield displacement of the equal area bilinear model, $u^{*}{}_{EQ}$, is estimated by balancing areas A1 and A2. This can be calculated as

$$u^{*}{}_{EQ} = \frac{(\mu_{inner} - \mu)\ x\ u^{*}}{u^{*}\ x\left(\frac{1}{R_{eff\ outer}}\right) - \mu_{outer}} \tag{5}$$

The friction coefficient at $u^{*}{}_{EQ}$ is calculated as

$$\mu@u^{*}{}_{EQ} = \mu + u^{*}{}_{EQ}\ x\left(\frac{1}{R_{eff\ outer}}\right) \tag{6}$$

The initial stiffness of the SDOF model, $k_{i,}$ is calculated using the previous results:

$$k_i = P_{Avg}\ x\left(\frac{\mu@u^{*}{}_{EQ}}{u^{*}{}_{EQ}}\right) \tag{7}$$

P_{avg} = Average load on an isolator

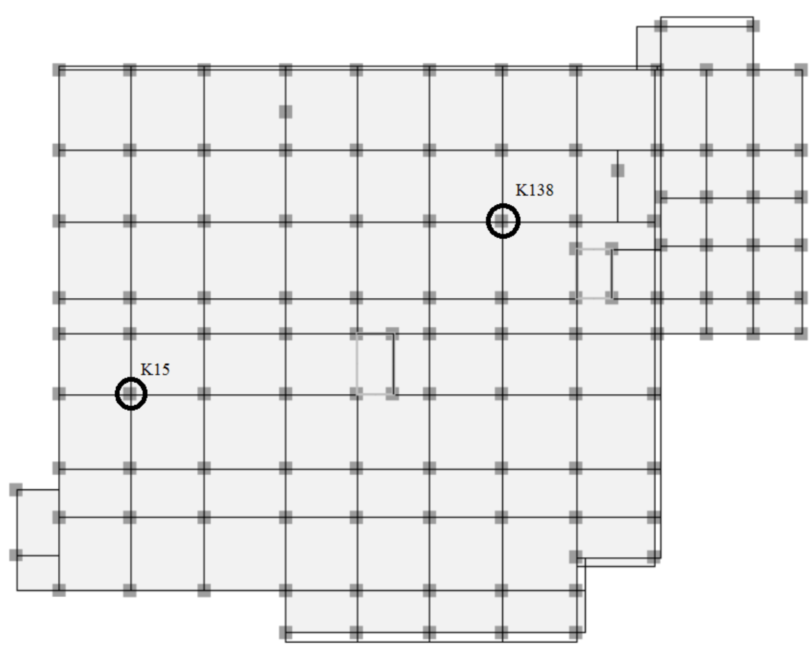

Fig.1 – A 2D view of the hospital of Piura and the location of the TFP and LRB system

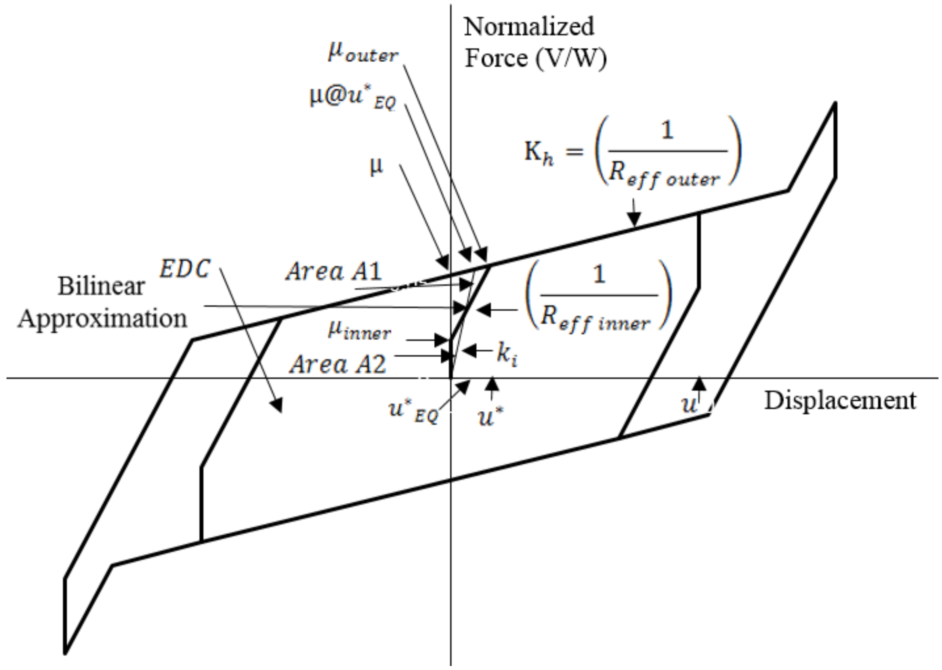

Fig.2 – Comparison of the true bearing behavior and the equal area bilinear approximation

2.2.3 Effective Stiffness (Horizontal)

As described in the CSI analysis reference manual, effective link stiffness is primarily used for linear analysis and response spectrum analysis. However, it is also used to generate the damping matrix for FNA time – history cases. To avoid introducing extraneous damping into cases of FNA analysis, it is recommended that the engineer set the effective stiffness to a very low value that will still permit the analysis to be run.

Effective Stiffness = 1 k – in (assumed)

2.2.4 Vertical Stiffness

The vertical stiffness of the link element is estimated as a linear spring. The stiffness of the spring is assumed to correspond to an imaginary steel cylinder within the isolator, with a cross-sectional area equal to the smallest diameter of any part of the isolator (A) and a height equal to the total height of the total isolator (L).

$$k_{Vertical} \approx E\ x \left(\frac{A}{L}\right) \tag{8}$$

2.2.5 Rotational Inertia

The rotational inertia of the link element has a negligible effect on the analysis results but can be important for analysis convergence. The rotational inertia of the isolator is estimated as a solid disk with a radius equal to the isolator.

$$I_z \approx \frac{m}{2} r^2 \tag{9}$$

$$I_x \approx I_y = \frac{m}{4} r^2 \tag{10}$$

Rotational mass at local axes 1, 2 and 3 are 0.5, 0.25 and 2.5 tonf-m2. The effective stiffness and non-linear stiffness in the axial direction (U1) is 215 x 10^4 kN/m, while the effective damping is considered 0 kN-s/m because damping is assumed to be contributed to by hysteresis and modal damping only, thus no added damping is included in the link element definition for all directions (U1, U2 and U3). The properties of the elements in the other two directions are shown in Table 1. Linear effective stiffness is set to 1 k-in or 180 kN-m for non-linear analysis to ensure proper construction of the damping matrix for the analysis in SAP2000.

Table 1 – U2 and U3 direction properties

U2 and U3 Properties						
Bound	Linear Properties	Non-Linear Properties				
	Effective Stiffness (kN/m)	Initial Stiffness (10^3) (kN/m)	Friction (Slow)	Friction (Fast)	Rate Parameter (sec/m)	Radius of sliding Surface (m)
Upper	180	7.8	0.060	0.120	50	4.25
Lower	180	9.0	0.043	0.086	50	4.25

2.3 Lead Rubber Bearing (LRB) System

This study incorporated a link element called the “rubber isolator,” which is used by the SAP2000 program to create a bilinear behavior of the LRB system. Analysis was carried out taking into account the properties of upper-bound and lower-bound isolators. The assumptions for modeling the LRB system were implemented in accordance to the IBC-SEAOC Structural /Seismic Design Manual [7] and are as follows:

To start the process of undertaking a prior analysis of this kind of isolation system, it is important for the engineer to have a good initial estimate of the desired isolator properties and resulting system displacement (Δ) for the Maximum Considered Earthquake. A good starting point for typical lead rubber bearing systems is to use an effective damping (β_{eff}) and an effective period (T_{eff}). By manipulating the design spectrum for these various levels of damping and looking at the displacement spectrum over the typical period range, the designer can define a range of target values.

With a target value of Δ, T_{eff} and β_{eff}, it is possible to iterate the isolation system properties by varying the values bearing yield strength (Q_d) and yielded stiffness(K_2). The values should be iterated until the resulting calculated T_{eff} and β_{eff} for the isolation system at Δ match the assumed starting values of T_{eff} and β_{eff} that define Δ: this can be viewed in figure 3.

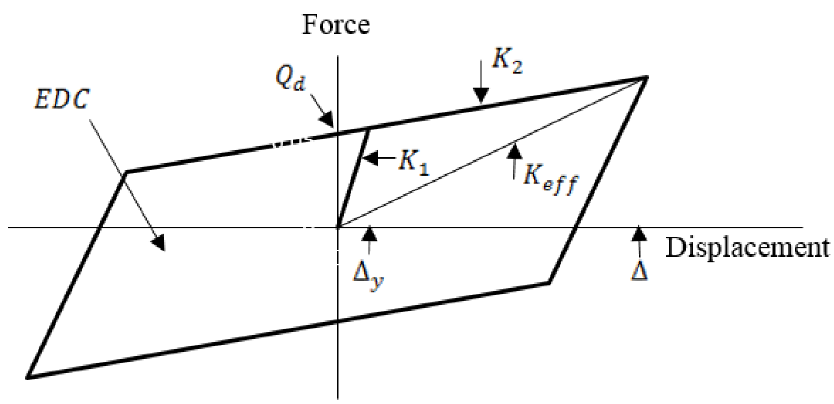

Fig.3 Force – definitions of the displacement isolation system

These terms can be calculated by using the following relationship from equation 12 to 19 [8]

$$K_1 = \frac{K_2}{0.08} \tag{11}$$

$$K_{eff} = \frac{Q_d}{\Delta} + K_2 \tag{12}$$

$$T_{eff} = 2\pi\, x \sqrt{\frac{W/g}{K_{eff}}} \tag{13}$$

$$\Delta_y = \frac{Q_d}{(K_1 - K_2)} \tag{14}$$

$$EDC = 4Q_d(\Delta - \Delta_y) \tag{15}$$

$$\beta_{eff} = \frac{EDC}{2\pi K_{eff\,\Delta^2}} \tag{16}$$

$$K_2 = \frac{GA_e}{T_r} \quad , \quad A_e = A - A_p \tag{17}$$

$$Q_d = F_y A_p \tag{18}$$

$$K_v = \frac{E_v A_b}{T_r} \tag{19}$$

The terms of K_1 (elastic stiffness), K_{eff} (effective stiffness), K_v (vertical stiffness), W (average load on an isolator), Δ_y (yielded displacement), EDC (area of hysteresis loop), G (effective shear modulus of rubber), A (gross area of rubber bearing), A_p (area of lead plug), A_b (gross bonded area of rubber bearing), T_r (total thickness of rubber), F_y= yield strength of lead and E_v (vertical stiffness modulus of isolator) describe equation from 12 to 19.

The output values from the study will provide the desired bearing yield strength value and yielded stiffness. The properties of a lead-rubber bearing can be calculated based on the construction of the bearing [8]. The diameter of the bearing and the number and thickness of rubber layers determine the stiffness of the bearing, while the diameter of the lead plug defines yield strength.

Table 2 – U2 and U3 direction properties

U2 and U3 Properties					
Type of LRB	Bound	Linear Properties	Non-Linear Properties		
		Effective Stiffness (kN/m)	Stiffness (10^3) (kN-m)	Yield Strength	Post Yield Stiffness Ratio
LRB-1	Upper	180	8	120	0.1
	Lower	180	5	80	0.1
LRB-2	Upper	180	9	220	0.1
	Lower	180	6	130	0.1

LRB-3	Upper	180	5.5	180	0.1
	Lower	180	4	120	0.1

The effective damping is considered 0 kN-s/m because damping is assumed to be contributed to by hysteresis and modal damping only. As a result, no added damping is included in the link element definition for all directions (U1, U2 and U3). The linear effective stiffness is set to 1 k-in or 180 kN-m for the non-linear analysis to ensure proper construction of the damping matrix for analysis in SAP2000. At the axial direction, the effective stiffness was considered 1.3, 1.9 and 0.8 x 10^6 kN-m for each link of the rubber element, respectively. The properties of the link elements in the other two directions are shown in Table 2.

3. Ground motion input

3.1 Ground Motion selection

In this paper, ground motions records were taken from "LRFD-based Analysis and Design Procedures for Bridge Bearings in Seismic Isolators" [9]. The ground motion records were applied to the model in the X and Y directions as shown in Figure 4.

The ground motion selection was performed according to the following considerations: the motions were to have near-fault characteristics; the Galzy record is from a backward-directivity region and all other records are from forward-directivity regions; the moment magnitudes for the motions are among 6.7 and 7.1; the site to source distances (Campbell R distance) are between 3 and 12 km; the records are from Site Classes C and D, Gazly and Loma Prieta are considered standard records with high frequency; Northridge and Kobe earthquakes are impulsive and are considered due to their proximity to fault lines; and the Turkey earthquake was included because it was highly destructive. Table 3 describes the peak ground acceleration (PGA), the peak ground velocity (PGV) and the peak ground displacement (PGD) for each ground motion.

3.2 Ground motion records scaling

Seven pairs of ground motion records were selected and scaled to represent the Peruvian response spectrum in accordance to E.030 [1], the Weighted Scaling methodology was used in accordance with ASCE 7-10 [10], Pant et al. [11]and Kumar et al. [12].

EQ_i	Event	Year	M_W [1]	R_{rup} [2] (km)	Site[3]	Fault Normal (FN) component			Fault Parallel (FP) component		
						PGA (g)	PGV cm/s	PGD (cm)	PGA (g)	PGV cm/s	PGD (cm)
1	Gazli, USSR	1976	6.69	5.46	C	0.60	64.8	24.1	0.71	70.9	24.8
2	Loma Prieta	1989	6.93	3.88	C	0.94	96.8	62.6	0.54	72.1	30.5
3	Loma Prieta	1989	6.93	9.31	C	0.40	71.2	20.8	0.26	59.9	29.8
4	Northridge	1994	6.69	5.43	C	0.52	67.6	42.1	1.07	64.6	21.1
5	Northridge	1994	6.69	5.19	C	0.84	116	39.3	0.49	78.2	29.9
6	Kobe, Japan	1995	6.90	3.00	D	0.65	72.6	20.8	0.70	83.2	26.7

7	Duzce,	1999	7.14	12.4	D	0.78	55.1	22.7	0.78	62.6	13.6

The code requires ground motion records scaled in a period interval from 0.5 TD to 1.25 TM [10]. This often requires an estimate of the period of the isolated structure. In view of this, a wider range of periods was used to ensure the suitability of the ground motions for both systems. For this study, the period interval for structural response has been estimated to be between 1.8 and 5.0 s.

Figure 4 presents the average of the 7 square root of sum of squares (SRSS) spectrum with Design Based Earthquake (DBE) spectrum E.030 and Maximum Considerable Earthquake (MCE or MCER) spectra for soil type S3. It corresponds to a point before the final scaling process for FN and FP components, while Figure 5 shows the response spectrum of the records at the end of the scaling process.

Table 3 - List the 7 pairs of ground motions selected for the preliminary analysis

1: Moment Magnitude.

2: Campbell R distance.

3: Site class classification per 2010 AASHTO Specifications.

4. Time History Analysis

4.1 Orientation of Ground Motion Records (FN & FP)

Figure 6 presents two orientations of the application direction of bidirectional FN and FP earthquake ground motion records for the building, taking into account the participation of 100% (FP) + 100% (FN) in case A, the participation of 100% (FN) + 100% (FP) in case B, -100% (FP) - 100% (FN) in case C and the participation of -100% (FN) - 100% (FP) in case D. Using the average definition of seismic hazard, all response parameters of interest were determined from the maximum of the average responses from the four orientation analyses for the Maximum Considered Earthquake.

4.2 Considerations of Time History Analysis

For this study, linear-elastic frames, shell elements and nonlinear link elements were considered for the model, and initial dead load under analysis was applied to the structure using a ramp function with a gradual load for the isolators applying 1g of acceleration downwards with a ramp function. The study also used an assumed mass source for specified load patterns as follows: 1.0 (dead load) + 0.5 (live load), the selection of damping ratio was defined as 2% for all modes, 0% in the first 3 isolated modes using modal overwrites, and the number of modes used in the analysis being 200. A Fast Nonlinear Analysis method was selected due to its computational speed and accuracy [13].

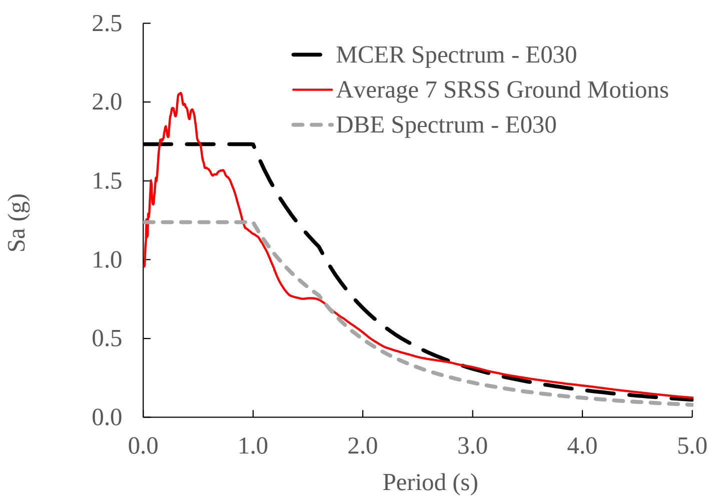

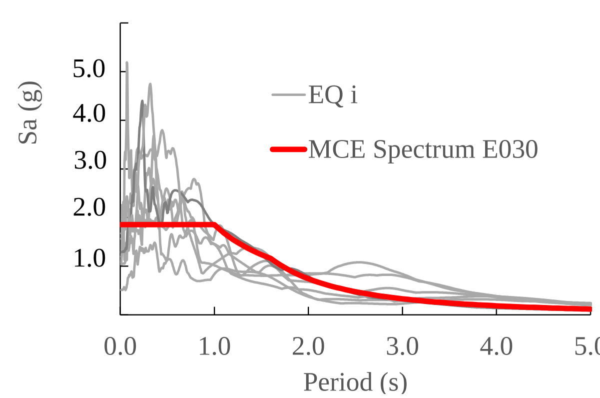

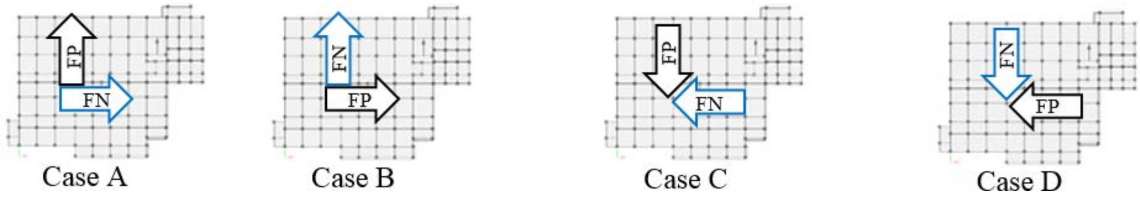

Fig.6 - Earthquake loading direction

5. Analysis Result

Results were obtained based on the average of seven pairs of ground motions in order to evaluate the response of the superstructure. The ground motions are depicted in Table 3. The isolator response was evaluated in term of hysteresis loops.

5.1 Average floor acceleration

It was found that the LRB System and TFP System performed well with respect to average floor acceleration response, taking into account seven pairs of ground motions. When undertaking the lower-bound analysis, the LRB System registered lower values of average floor accelerations compared to the TFP System, while the TFP System recorded a lower response of average floor accelerations compared to the LRB System when subjected to upper bound analysis, as detailed in Table 4.

Figure 7 presents the floor acceleration response for the Loma Prieta earthquake at first and fifth floor level for both systems of upper bound analysis and the floor acceleration response for the Kobe earthquake in Japan at first and fifth floor level for both systems of lower bound analysis. These analyses were carried out taking into account case A earthquake loading direction.

Table 4 – Average on first and fifth floor acceleration

Earthquake Loading Direction	Average first floor acceleration (g)				Average fifth floor acceleration (g)			
	LRB		TFP		LRB		TFP	
	LB	UB	LB	UB	LB	UB	LB	UB
Case A	0.32	0.46	0.36	0.40	0.53	0.69	0.62	0.67
Case B	0.34	0.44	0.40	0.44	0.50	0.69	0.58	0.67
Case C	0.32	0.46	0.30	0.42	0.53	0.68	0.54	0.65
Case D	0.35	0.43	0.41	0.48	0.51	0.69	0.57	0.62

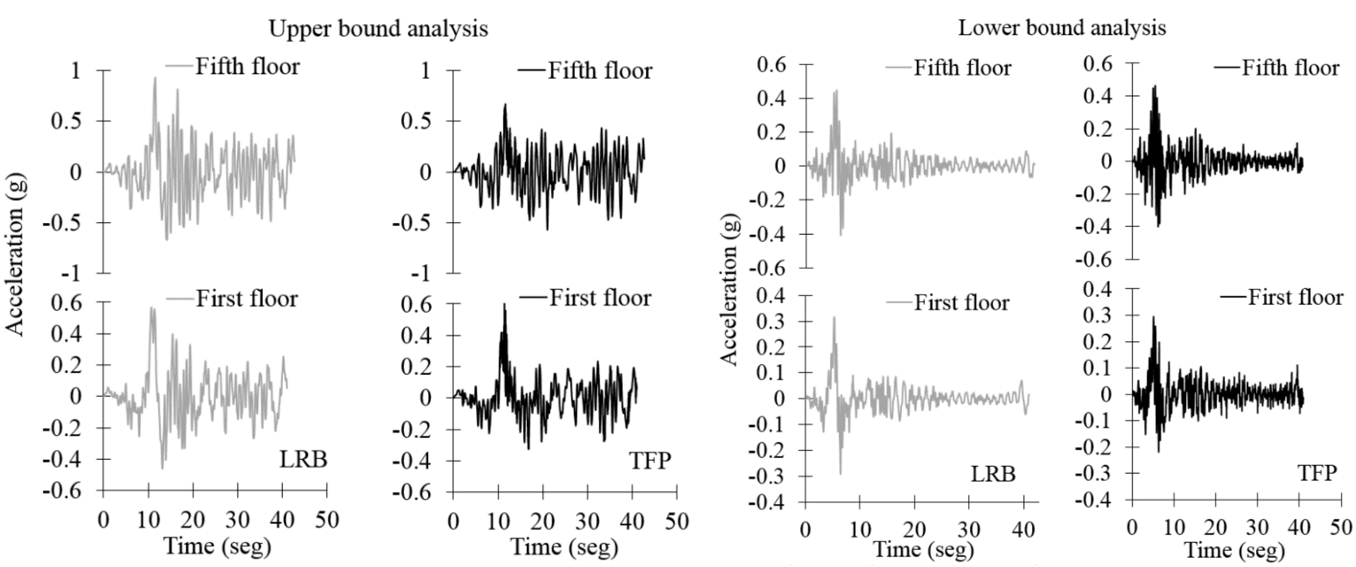

Loma Prieta earthquake Kobe earthquake

Fig.7 - Floor acceleration response

Table 5 – Average on first and fifth inter-story drift

Earthquake Loading Direction	Average first inter-story drift (1/1000)				Average fifth inter-story drift (1/1000)			
	LRB		TFP		LRB		TFP	
	LB	UB	LB	UB	LB	UB	LB	UB
Case A	5.65	6.88	4.41	4.70	1.52	1.93	1.32	1.59
Case B	6.00	6.87	4.67	4.83	1.61	1.91	1.43	1.55
Case C	5.65	6.89	4.39	4.66	1.53	1.93	1.32	1.57
Case D	5.99	6.87	4.60	4.81	1.57	1.91	1.42	1.59

Table 6 – Average base shear

Earthquake loading direction	Average base shear (kN) x 1.00E+04			
	LRB		TFP	
	LB	UB	LB	UB
Case A	5.60	7.05	4.65	4.80
Case B	6.10	7.15	4.90	4.95
Case C	5.60	7.05	4.60	4.95
Case D	6.15	7.15	4.85	4.90

5.2 Average inter-story Drift

Average inter-story drift was carried out in the center of mass of each floor. For lower bound analysis and for upper bound analysis, the TFP System recorded better conduct for the LRB System, with both systems based on E030 [1], as indicated in Table 5.

5.3 Average base shear

The TFP System registered lower average base shear compared to the LRB System, which was around 20% for lower bound analysis and 30% for upper bound analysis, as indicated in Table 6.

5.4 Isolator response

Isolator response was carried out using lower and upper bound analysis focusing on the hysteresis loops. A study was made of the hysteresis conduct of isolators K-15 and K-138, as shown in Figure 1. The hysteresis loops of isolator K-15 for both analyses with respect to the Kobe earthquake in Japan are shown in Figure 8, while the hysteresis loops of isolator K-138 for both analyses with respect to the Loma Prieta earthquake are shown in Figure
9.

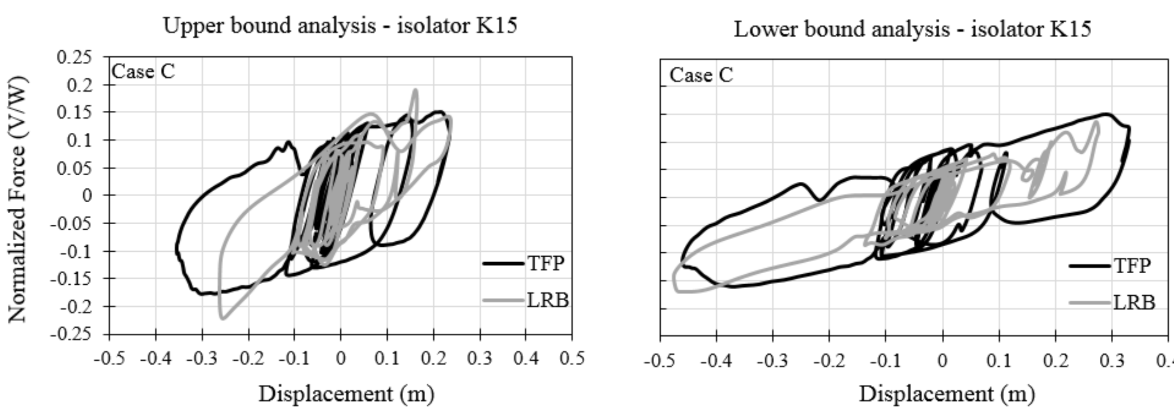

Fig.8 – Normalized force vs. Isolation layer displacement Hysteresis, Kobe earthquake

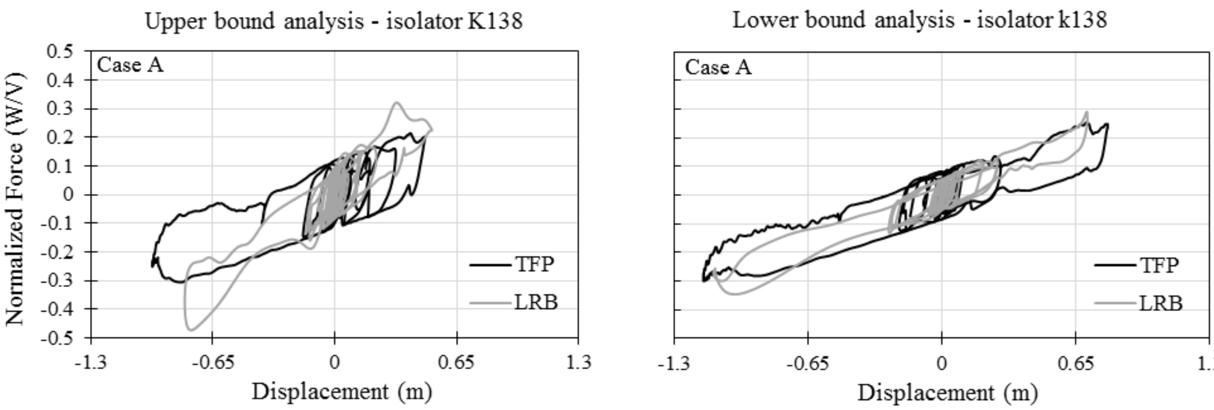

Fig.9 – Normalized force vs. Isolation layer displacement Hysteresis, Loma Prieta earthquake

In the case of these isolators, there is a tendency of improved behavior in the LRB Systems with respect to the normalized shear force compared to the TFP Systems for lower bound analysis, while in the case of upper bound analysis, the TFP Systems register improved behavior in accordance to the normalized shear force.

For both analysis, and with respect to isolators K-15 and K-138, the area of hysteresis loop (energy of dissipation) was greater in the TFP Systems compared to the LRB Systems.

6. Conclusions

A nonlinear analysis was carried out in order to evaluate the performance of two isolation systems. The analysis was carried out according to the specifications of the IBC SEAOC Structural / Seismic Design Manual, volume 5 – Examples for Seismically Isolated Buildings and Buildings with Supplemental Damping. Based on this analysis, the following conclusions can be drawn.

It was found that the LRB System and TFP System performed well for average floor acceleration response, taking into account the seven pairs of ground motions. When undertaking the lower bound analysis, the LRB System had lower values of average floor accelerations than the TFP System, while the TFP System had a lower response of average floor accelerations than the LRB System for undertaking upper bound analysis. The floor acceleration response for the Loma Prieta earthquake was the highest: in the case of LRB System, the value was 9.8 m/s2 and in the case of TFP System it was 10.5 m/s2. However, the floor acceleration response for the Kobe earthquake in Japan was the lowest: in the case of the LRB System the value was 2.3 m/s2 and in the case of the TFP System it was 1.9 m/s2.

The results of inter-story drift as an average of the seven pairs of ground motions in both systems were based on E030. The Loma Prieta earthquake's inter-story drift response was the highest. In the case of the LRB System the value was 0.012146 and in the case of the TFP System it was 0.00826. For the Kobe earthquake in Japan the inter-story drift response was the lowest. In the case of the LRB System the value was 0.000996 and in the case of the TFP System it was 0.000912.

On average, base shear for the TFP system was lower than the LRB system (around 30%); however, base shear demand would not be relevant in the seismic response.

The response of non-lineal analysis on isolators as hysteresis loops in both seismic isolation devices was determined using a bilineal model. On average, for lower bound analysis, the LRB Systems had lower shear force and displacements than the TFP Systems. However, for upper bound analysis, TFP Systems had a lower shear force and a greater displacement than the LRB Systems.

To sum up, LRB Systems provided a better average floor acceleration response and hysteresis loops than the TFP Systems for undertaking lower bound analysis, while the TFP Systems had better average floor acceleration response and hysteresis loops than the LRB Systems for undertaking upper bound analysis.

7. References

[1] Peruvian Earthquake Resistant Code (2016): Earthquake Resistant design E-030, Peru. (In Spanish)

[2] Skinner I, Robinson H and Graeme H (1993): An Introduction to Seismic Isolation. Wiley, 1st edition.

[3] Kenneth R, Valencia A (2000): Machu Picchu, a Civil Engineering Marvel, ASCE.

[4] AASHTO Guide Specifications for Seismic Isolation Design (2010).

[5] Fenz, DM, and Constantinou MC (2008): Spherical Sliding Isolation Bearings with adaptive behavior: Theory *Earthquake Engineering and Structural Dynamics* **37**, 163-183.

[6] CSI Computer & Structures INC, SAP2000 15.0.0 (2014)

[7] 2012 IBC, SEAOC Structural/ Seismic Design Manual (2013), volume 5: Examples for Seismically Isolated Building and Building with Supplemental Damping.

[8] Farzad Naeim, James M. Kelly (1999): Design of Seismic Isolated Structures from theory to practice.

[9] Constantinou MC, Kalpakidis I, Filiatrault A and Ecker L (2011): LRFD-based Analysis and Design Procedures for Bridge Bearings in Seismic Isolators, MCEER-11. *Technical Report MCEER 2011/09*, Multidisciplinary Center for Earthquake Engineering Research.

[10] American Society of Civil Engineers (2010): Minimum Design Loads for Buildings and Other Structures, ASCE Standard ASCE/SEI 7-10, Reston, VA, USA

[11] Deepak RP, Constantinou MC, Wijeyewickrema A (2013): Re-evaluation of equivalent lateral force procedure for prediction of displacement demand in seismically isolated structures. *ELSEVIER*, *Engineering Structures* **52**, 455-465.

[12] Kumar M, Whittaker AS and Constantinou MC (2015): Seismic Isolation of Nuclear Power Plants using Sliding Bearings, MCEER-15-006. *Technical Report MCEER 2015/06*, Multidisciplinary Center for Earthquake Engineering Research.

[13] Constantinou MC (2015): Class Notes of Seismic Isolation CIE 625, University at Buffalo.